ChemComm

COMMUNICATION

View Article Online
View Journal | View Issue

Cite this: *Chem. Commun.*, 2018, **54**, 5342

Received 12th March 2018,
Accepted 24th April 2018

DOI: 10.1039/c8cc01974f

rsc.li/chemcomm

A novel strategy to evaluate the degradation of quantum dots: identification and quantification of CdTe quantum dots and corresponding ionic species by CZE-ICP-MS†

Peijun Meng,[ab] Yamin Xiong,[ac] Yingting Wu,[d] Yue Hu,[ac] Hui Wang,[ac] Yuanfeng Pang,[ac] Shuqing Jiang,[ac] Sihai Han[e] and Peili Huang *[ac]

In view of the significance and urgency of the speciation analysis of quantum dots (QDs) and their degradation products for clarifying their degradation rules and toxicity mechanisms, a method for the identification and quantification of CdTe QDs and corresponding ionic species in complex matrices was developed using capillary zone electrophoresis (CZE) coupled to inductively coupled plasma-mass spectrometry (ICP-MS). The quality assessment of commercial CdTe QDs and serum pharmacokinetics of synthesized CdTe QDs in rats were successfully undertaken using the developed CZE-ICP-MS method.

Quantum dots (QDs) exhibit special physicochemical properties and unique optical properties and have been widely applied in biomedical imaging, biological sensing and chemical detection,[1–6] *etc.* As a result, environmental and biological exposure to QDs has become increasingly prominent, and their potential risks to human health and the environment, especially those of Cd-based QDs, are becoming an important topic.

The release of free Cd^{2+} resulting from the degradation of Cd-based QDs has been suggested to be the cause of their overall toxicity in organisms.[7–9] Traditional methods for evaluating the degradation of QDs mainly include blue shifts in spectra (fluorescence excitation spectra and UV-visible absorption spectra),[7] the decrease of fluorescence intensity and tissue metallothionein (MT) elevation (free Cd^{2+} is a potent inducer of MT),[8,10] *etc.* However, these methods have been deemed to be problematic due to either the aggregation of QDs or the high and variable background fluorescence that results from the complex media or the fact that these methods cannot accurately quantify the QDs. A variety of on-line combined techniques, such as size exclusion chromatography (SEC) coupled with inductively coupled plasma-mass spectrometry (ICP-MS),[11,12] thin layer chromatography (TLC) coupled to ICP-MS,[13] field flow fractionation (FFF) coupled to ICP-MS,[14] *etc.*, have been widely used for the quantification of nanoparticles (NPs) and corresponding metal ions. However, the above methods are either poorly reproducible with weak separation abilities, give low recovery rates or are unable to achieve simultaneous detection of NPs and ions.

Capillary electrophoresis (CE) combined with ICP-MS provides extremely high sensitivity for small sample volumes and has exhibited great potential for the characterization and separation of NPs, including AgNPs,[15] AuNPs,[16] *etc.* However, due to the strong adsorption of QDs to ions[17] and the complexity of CE, the simultaneous separation and accurate quantification of QDs and corresponding ionic species is very difficult and has not been reported so far.

In this study, CdTe QDs capped with L-glutathione/L-cysteine were synthesized and selected as the research target in view of their wide applications,[18] convenient preparation by an aqueous "green" route and their high fluorescence quantum yields (Fig. 1). During the degradation of Te-containing QDs under certain conditions, Te can be released and could be further oxidized to form the oxyanion TeO_3^{2-}, which is highly toxic to most

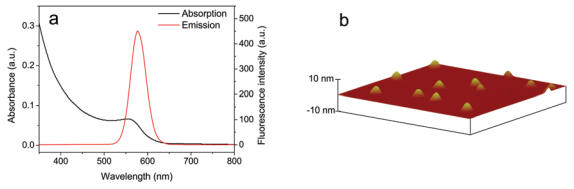

Fig. 1 Absorption spectra and emission spectra (a) and AFM image (b) of L-GSH/L-Cys-capped CdTe QDs obtained in aqueous solution. The maximum emission wavelength is 580 nm (λ_{ex} = 450 nm), with a full width at half-maximum (FWHM) of the fluorescence emission spectra of 42 nm. The average diameter of CdTe QDs was 5.1 ± 0.6 nm.

[a] *School of Public Health, Capital Medical University, Beijing 100069, China. E-mail: huangpl@ccmu.edu.cn*
[b] *Public Health School, Baotou Medical College, Inner Mongolia University of Science & Technology, Baotou 014060, China*
[c] *Beijing Key Laboratory of Environmental Toxicology, Beijing 100069, China*
[d] *Core Facility Center, Capital Medical University, Beijing 100069, China*
[e] *College of Food and Bioengineering, Henan University of Science and Technology, Luoyang 471023, China*

† Electronic supplementary information (ESI) available: Experimental section, additional figures and tables. See DOI: 10.1039/c8cc01974f

microorganisms.[19,20] We developed the capillary zone electrophoresis coupled to ICP-MS (CZE-ICP-MS) method for the separation and quantification of CdTe QDs and corresponding ionic species (Cd^{2+} and TeO_3^{2-}) in buffer solution and complex biological matrices for the first time.

Firstly, we optimized the separation conditions of CdTe QDs, Cd^{2+} and TeO_3^{2-}. Considering the stability of CdTe QDs and the electro-osmotic flow (EOF), the pH values of the running buffer and sample buffer were adjusted to 8.0–10.0 in the following studies. We found that the separation of CdTe QDs and TeO_3^{2-} in buffer solution was realized successfully with a borate saline buffer (BSB, $Na_2B_4O_7$–H_3BO_3, pH 9.0) as the running buffer and a phosphate buffer (PB, Na_2HPO_4–NaH_2PO_4, pH 8.0) as the sample buffer. However, no isolated Cd^{2+} peak was observed, as the migration time (t_M) of Cd^{2+} is consistent with that of CdTe QDs (Fig. 2a and b). In addition, the results show no improvement when both the running buffer and the sample buffer are either PB or BSB with different pH values (Fig. S1 and S2, ESI†). We tried to realize the separation of CdTe QDs and Cd^{2+} by adding sodium dodecyl sulfate (SDS, anionic surfactant), cetyltrimethyl ammonium bromide (CTAB, cationic surfactant), or Tween 20 (nonionic surfactant) to the running buffer and/or the sample buffer. Moreover, the addition of ethylenediamine tetraacetic acid (EDTA) to the sample solution leads to the formation of a small molecular Cd^{2+}–EDTA complex[11] which changes the charge-to-size ratio. The results showed no change in the elution of CdTe QDs and Cd^{2+} in the above work.

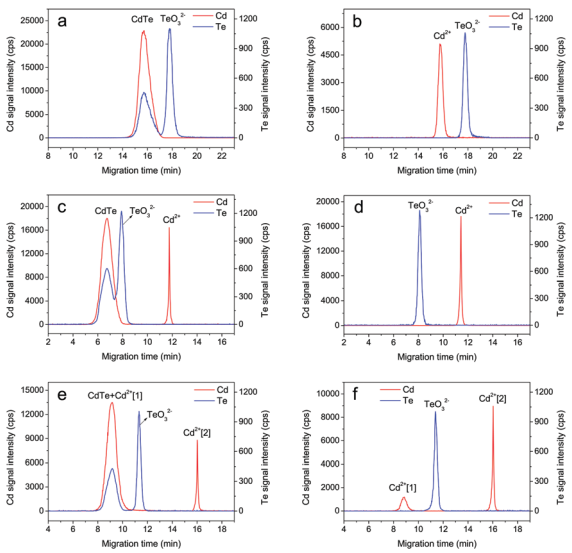

Fig. 2 Electropherograms of (a, c and e) the mixture sample consisting of 40 μM CdTe QDs (calculated as Cd, the same as below), 0.5 mg L^{-1} Cd^{2+} and 0.5 mg L^{-1} TeO_3^{2-} (calculated as Te, the same as below) in buffer solution obtained using CZE-ICP-MS. Electropherograms of (b, d and f) the mixture sample consisting of 0.5 mg L^{-1} Cd^{2+} and 0.5 mg L^{-1} TeO_3^{2-} in buffer solution obtained using CZE-ICP-MS. (a and b) The running buffer is 40 mM BSB (pH 9.0). 30 mM PB (pH 8.0) was added to the sample solution. (c and d) The running buffer is 30 mM Na_2HPO_4 (pH 9.0). 0.3% (v/v) Tween 20 and 40 mM BSB (pH 9.0) were added to the sample solution. (e and f) The running buffer is 30 mM Na_2HPO_4 (pH 9.0). 2 mg mL^{-1} HSA and 40 mM BSB (pH 9.0) were added to the sample solution.

However, when 30 mM Na_2HPO_4 (pH 9.0) and BSB (pH 9.0) were used as the running buffer and the sample buffer respectively, we found that the t_M of Cd^{2+} gradually moved backwards compared with that of TeO_3^{2-} with the increase in the BSB concentration. Adding 0.3% (v/v) Tween 20 to the sample solution could dramatically improve the stability of the electrophoretic current, thereby improving the reproducibility. The Cd^{2+} peak completely moved to the back of the TeO_3^{2-} peak and baseline separation was realized when the concentration of BSB (pH 9.0) reached 40 mM (Fig. S3, ESI†). This interesting phenomenon can probably be attributed to the formation of a Cd^{2+}–BSB complex with a larger negative charge, which migrates faster than TeO_3^{2-} in the opposite direction of the EOF, and thus elutes at a later time compared to TeO_3^{2-}. Therefore, in subsequent studies, 40 mM BSB (pH 9.0) was selected as the optimal sample buffer. Unfortunately, under current separation conditions, the Cd^{2+} was thoroughly separated from the CdTe QDs, but baseline separation of the CdTe QDs and TeO_3^{2-} was not achieved (Fig. 2c and d). Later, we added human serum albumin (HSA) to the sample solution, and were surprised to find that not only could HSA play the same role as Tween 20 in improving the electrophoretic current stability but the addition also realized the baseline separation between CdTe QDs, Cd^{2+} and TeO_3^{2-} (Fig. 2e). Nevertheless, in the electropherogram of Cd^{2+} and TeO_3^{2-} (Fig. 2f), two distinct peaks due to Cd^{2+} species were observed, and the shorter t_M of the Cd^{2+} species peak was identical to that of the CdTe QDs in Fig. 2e. These two Cd^{2+} species with the shorter t_M and the longer t_M compared with TeO_3^{2-} were named Cd^{2+}[1] and Cd^{2+}[2], respectively. It was speculated that Cd^{2+}[1] was probably a Cd^{2+}–HSA complex,[21,22] which has a similar charge-to-size ratio to the CdTe QDs and the Cd^{2+}[2] was probably a Cd^{2+}–BSB complex.

Furthermore, the influence of the HSA concentration on the separation and method sensitivity of CdTe QDs, Cd^{2+} and TeO_3^{2-} was studied in the range of 0–5 mg mL^{-1} (Fig. S4, ESI†).

The results indicated that the resolution of Cd^{2+} and TeO_3^{2-} was improved with the increase in the HSA concentration, and the signal intensity of the peak due to Cd^{2+}[1] was enhanced when the HSA concentration was increased; however, the opposite trend was observed for Cd^{2+}[2]. The total signal intensities of Cd^{2+}[1] and Cd^{2+}[2] remained unchanged, which means that these two Cd^{2+} species have the same vaporization and diffusion effects according to CZE-ICP-MS analysis. In addition, with a fixed HSA concentration, the peak area ratio of Cd^{2+}[1] to Cd^{2+}[2] stays almost constant and does not change with the Cd^{2+} concentration in solution. Therefore, the Cd^{2+}[2] signal was used as the basis in the following quantification analysis of the Cd^{2+} containing the Cd^{2+}[1] and Cd^{2+}[2] species. Considering the adequate resolution between CdTe QDs and TeO_3^{2-}, 2 mg mL^{-1} HSA was adopted as the optimum additive concentration.

Additionally, under the current optimum conditions, the influence of the concentration of Na_2HPO_4 (pH 9.0) as the running buffer on the separation of CdTe QDs, Cd^{2+} and TeO_3^{2-} was investigated using CZE-ICP-MS (Fig. S5, ESI†). Ultimately, 30 mM Na_2HPO_4 (pH 9.0) was selected as the optimal running buffer in all subsequent experiments.

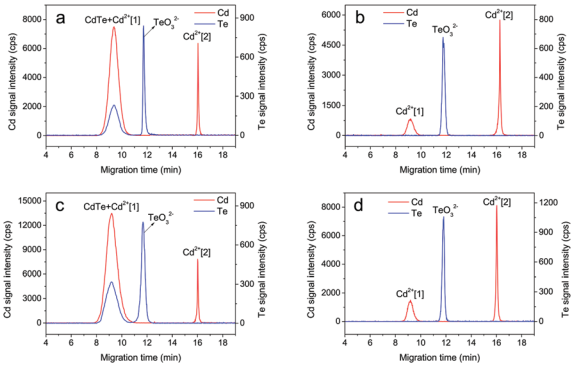

Fig. 3 Electropherograms of the mixture sample consisting of 40 μM CdTe QDs, 0.5 mg L^{-1} Cd^{2+} and 0.5 mg L^{-1} TeO_3^{2-} in the cell culture solution (a) and the serum sample (c) obtained using CZE-ICP-MS. Electropherograms of the mixture sample consisting of 0.5 mg L^{-1} Cd^{2+} and 0.5 mg L^{-1} TeO_3^{2-} in the cell culture solution (b) and the serum sample (d) obtained using CZE-ICP-MS. The running buffer is 30 mM Na_2HPO_4 (pH 9.0). 40 mM BSB (pH 9.0) was added to the sample solution.

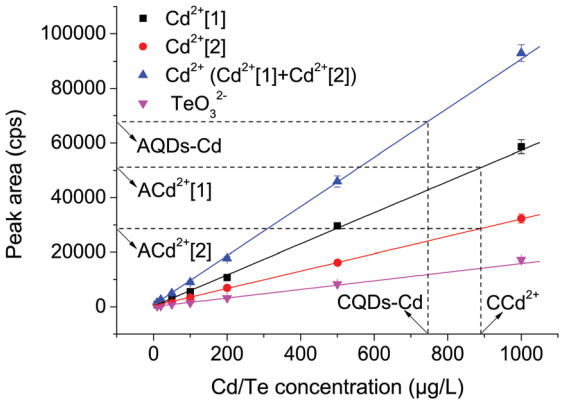

Fig. 4 Schematic of the simultaneous quantification of CdTe QDs, Cd^{2+} and TeO_3^{2-} in samples. $ACd^{2+}[1]$, $ACd^{2+}[2]$ and AQDs–Cd in this figure represent the peak areas of $Cd^{2+}[1]$, $Cd^{2+}[2]$ and Cd of the CdTe QDs, respectively. CCd^{2+} and CQDs–Cd represent the concentrations of the Cd^{2+} and Cd of the CdTe QDs in samples, respectively.

The speciation of CdTe QDs, Cd^{2+} and TeO_3^{2-} in the cell culture solution and serum sample was analyzed using CZE-ICP-MS. The results showed that the mixture was completely separated with satisfactory resolution (Fig. 3a and c). The Cd^{2+} peak was proportionally divided into peaks due to $Cd^{2+}[1]$ and $Cd^{2+}[2]$ (Fig. 3b and d). According to the previous experimental results, it is easy to speculate that $Cd^{2+}[1]$ might be a complex of Cd^{2+} and fetal bovine serum albumin (Cd^{2+}–FBSA) from the cell culture solution or the complex of Cd^{2+} and rat serum albumin (Cd^{2+}–RSA) from the serum sample, and $Cd^{2+}[2]$ was probably the Cd^{2+}–BSB complex.

For the separation of CdTe QDs, Cd^{2+} and TeO_3^{2-} in the cell culture solution, as discussed before, the $Cd^{2+}[2]$ signal increased with the concentration of fetal bovine serum (FBS). As a result, the cell culture solution containing 10% FBS was diluted twice as part of the optimum conditions, and the other optimum conditions were the same as above. For the separation of CdTe QDs, Cd^{2+} and TeO_3^{2-} in the serum sample, in order to obtain the maximum signal intensity of $Cd^{2+}[2]$ to improve the analysis sensitivity of the Cd^{2+} obtained from the CdTe QD degradation in serum samples, the dilution factor of the serum sample was optimized by the speciation analysis of Cd^{2+} in the serum sample (Fig. S6, ESI†). Ultimately, the serum sample was diluted 20 times as part of the optimum conditions. In addition, the peak area ratio of $Cd^{2+}[1]$ to $Cd^{2+}[2]$ remained constant with a fixed concentration of FBSA or RSA in the sample solution, which means that FBSA and RSA could play the same important role as HSA in the buffer solution.

Next, the analytical performance parameters of the CZE-ICP-MS method are evaluated and summarized in Table S2 (ESI†). The results were satisfactory with a wide linear range, low limits of detection (LODs, microgram per liter for TeO_3^{2-} and sub-microgram per liter for Cd^{2+}), good repeatability and good selectivity for the quantification of CdTe QDs, Cd^{2+} and TeO_3^{2-} in different matrices.

From the above results, it is clearly shown that the Cd^{2+} species were proportionally divided into $Cd^{2+}[1]$ and $Cd^{2+}[2]$ in three matrices, and the electrophoresis peak due to the CdTe QDs overlaps with that due to $Cd^{2+}[1]$. Therefore, the simultaneous quantification of CdTe QDs, Cd^{2+} and TeO_3^{2-} can be carried out according to the method shown in Fig. 4. Specifically, the Cd^{2+} was quantified by the external calibration curves of $Cd^{2+}[2]$. Then, in turn, the peak area of $Cd^{2+}[1]$ was deduced by the external calibration curves of $Cd^{2+}[1]$. For the quantification of Cd of the CdTe QDs (CdTe QDs–Cd), the peak area of CdTe QDs–Cd was calculated by subtracting the peak area of $Cd^{2+}[1]$ from the overlapping peak areas of CdTe QDs–Cd and $Cd^{2+}[1]$. Then, CdTe QDs–Cd was quantified using the external calibration curves of the Cd^{2+} species ($Cd^{2+}[1]$ + $Cd^{2+}[2]$). Furthermore, the TeO_3^{2-} and Te of the CdTe QDs (CdTe QDs–Te) in samples were quantified directly using the external calibration curves of TeO_3^{2-}. Additionally, the accuracy of the above quantitative methods was validated by quantitating the CdTe QDs with different sample pretreatment methods (Table S3, ESI†).

Lastly, the quality assessment of commercial CdTe QDs and serum pharmacokinetics of synthesized CdTe QDs in rats were successfully undertaken using the developed CZE-ICP-MS method. The electropherograms of two commercial CdTe QDs are shown in Fig. S7 (ESI†). The analysis results showed that commercial CdTe QDs exhibited severe degradation and/or the purification was not effective (Table S4, ESI†). Therefore, the quality evaluation of QDs before the animal/cell experiments is extremely necessary for toxicity mechanism studies of QDs. Fischer *et al.*[23] first tracked QDs *via* Cd measurement in the blood and organs of rats using inductively coupled plasma-atomic emission spectrometry (ICP-AES) and presented a quantitative report on the kinetic parameters of QDs in the rats. Several biological fate studies of QDs *in vivo* using ICP-AES and ICP-MS have since been reported.[24–26] However, the uncoupled ICP-AES and ICP-MS analytical techniques were unable to distinguish whether Cd was bound within the QDs or had been released into the blood or tissues. In this study, we accurately determined the amounts of CdTe QDs–Cd, CdTe QDs–Te,

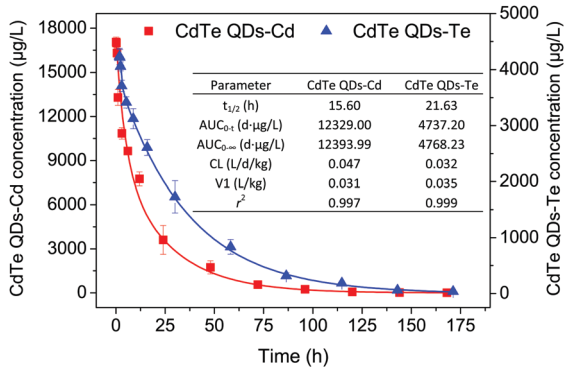

Fig. 5 Concentration–time curves of CdTe QDs–Cd and CdTe QDs–Te in rat serum after intravenous injection of synthesized CdTe QDs by CZE-ICP-MS analysis. $t_{1/2}$ is the elimination half-life time. AUC_{0-t} is the area under the serum concentration–time profiles between 0 and t days (t is 7 d for CdTe QDs–Cd and t is 6 d for CdTe QDs–Te). CL is the clearance rate. V_1 is the apparent distribution volume of the central compartment for the two-compartment model. r^2 is the square of the correlation coefficient of the fitting curve.

free Cd^{2+}, and TeO_3^{2-} in serum in a single run using the developed CZE-ICP-MS method. The concentration changes of CdTe QDs, Cd^{2+} and TeO_3^{2-} in serum with time are shown in Table S5 (ESI†). The simulated serum circulation curves and the main pharmacokinetic parameters calculated by fitting the data over 1 week with the two-compartment model are shown in Fig. 5. The results showed that the molar ratio of CdTe QDs–Cd to CdTe QDs–Te in serum was reduced from 4.50 ± 0.24 to 0.79 ± 0.37 (far below the initial molar ratio of 4.56 ± 0.38), which means the degradation rate of CdTe QDs–Cd is faster than that of CdTe QDs–Te. Further studies will be performed to understand the degradation or metabolism mechanisms of CdTe QDs, and this work is ongoing.

In summary, we have developed a promising method for the identification and quantification of CdTe QDs and their degradation products (Cd^{2+} and TeO_3^{2-}) in complex matrices using CZE-ICP-MS. The key to the successful separation is to utilize Na_2HPO_4 (pH 9.0) and $Na_2B_4O_7$–H_3BO_3 (pH 9.0), inexpensive and commonly used reagents, as the running buffer and the sample buffer, respectively. Furthermore, the addition of HSA to the buffer solution was considered necessary for the baseline separation of CdTe QDs and TeO_3^{2-}, and no additional reagents were required for the cell culture solution and animal serum due to the serum albumin coexisting in the above two complex matrices. The developed CZE-ICP-MS method has been successfully applied to the quality assessment of commercial CdTe QDs and the serum pharmacokinetics of synthesized CdTe QDs. The proposed method provides a novel strategy not only for comprehensively understanding the degradation rules and toxicity mechanisms of CdTe QDs but also for the study of the purification effect and synthetic process control of CdTe QDs. Furthermore, it also provides ideas for relevant research into other QDs and their analogues.

This work was supported by the National Natural Science Foundation of China (No. 81273131, 81573201, and 31471658), and the Beijing Natural Science Foundation Program and the Scientific Research Key Program of the Beijing Municipal Commission of Education (KZ201510025027).

Conflicts of interest

There are no conflicts to declare.

Notes and references

1 A. Fontes and B. S. Santos, *Quantum Dots: Applications in Biology*, Springer, New York, 2nd edn, 2014, pp. 3–8.
2 X. Michalet, F. F. Pinaud, L. A. Bentolila, J. M. Tsay, S. Doose, J. J. Li, G. Sundaresan, A. M. Wu, S. S. Gambhir and S. Weiss, *Science*, 2005, **307**, 538–544.
3 Y. Wang and X. P. Yan, *Chem. Commun.*, 2013, **49**, 3324–3326.
4 C. Li, T. Bai, F. Li, L. Wang, X. Wu, L. Yuan, Z. Shi and S. Feng, *CrystEngComm*, 2013, **15**, 597–603.
5 Y. Tang, X. Jiao, R. Liu, L. Wu, L. Wu, X. Hou and Y. Lv, *J. Anal. At. Spectrom.*, 2011, **26**, 2493–2499.
6 P. Wu and X. P. Yan, *Chem. Commun.*, 2010, **46**, 7046–7048.
7 A. M. Derfus, W. C. W. Chan and S. N. Bhatia, *Nano Lett.*, 2004, **4**, 11–18.
8 C. H. Lin, L. W. Chang, H. Chang, M. H. Yang, C. S. Yang, W. H. Lai, W. H. Chang and P. Lin, *Nanotechnology*, 2009, **20**, 215101.
9 M. Wang, J. Wang, H. Sun, S. Han, S. Feng, L. Shi, P. Meng, J. Li, P. Huang and Z. Sun, *Int. J. Nanomed.*, 2016, **11**, 2319–2328.
10 N. Liu, Y. Mu, Y. Chen, H. Sun, S. Han, M. Wang, H. Wang, Y. Li, Q. Xu, P. Huang and Z. Sun, *Part. Fibre Toxicol.*, 2013, **10**, 37–45.
11 L. Peng, M. He, B. Chen, Y. Qiao and B. Hu, *ACS Nano*, 2015, **9**, 10324–10334.
12 X. X. Zhou, R. Liu and J. F. Liu, *Environ. Sci. Technol.*, 2014, **48**, 14516–14524.
13 N. Yan, Z. Zhu, L. Jin, W. Guo, Y. Gan and S. Hu, *Anal. Chem.*, 2015, **87**, 6079–6087.
14 E. Bolea, J. Jiménez-Lamana, F. Laborda and J. R. Castillo, *Anal. Bioanal. Chem.*, 2011, **401**, 2723–2732.
15 L. Liu, B. He, Q. Liu, Z. Yun, X. Yan, Y. Long and G. Jiang, *Angew. Chem., Int. Ed.*, 2014, **53**, 14476–14479.
16 B. Franze and C. Engelhard, *Anal. Chem.*, 2014, **86**, 5713–5720.
17 W. Zhang, Y. Miao, K. Lin, L. Chen, Q. Dong and C. Huang, *Environ. Pollut.*, 2013, **176**, 158–164.
18 C. Carrillo-Carrión, S. Cárdenas, B. M. Simonet and M. Valcárcel, *Chem. Commun.*, 2009, 5214–5226.
19 A. Ramos-Ruiz, J. A. Field, J. V. Wilkening and R. Sierra-Alvarez, *Environ. Sci. Technol.*, 2016, **50**, 1492–1500.
20 R. J. Turner, J. H. Weiner and D. E. Taylor, *Microbiology*, 1999, **145**, 2549–2557.
21 Q. Xiao, S. Huang, W. Su, P. Li, J. Ma, F. Luo, J. Chen and Y. Liu, *Colloids Surf., B*, 2013, **102**, 76–82.
22 L. Lai, J. C. Jin, Z. Q. Xu, P. Mei, F. L. Jiang and Y. Liu, *Chemosphere*, 2015, **135**, 240–249.
23 H. C. Fischer, L. Liu, K. S. Pang and W. C. W. Chan, *Adv. Funct. Mater.*, 2006, **16**, 1299–1305.
24 R. S. H. Yang, L. W. Chang, J. P. Wu, M. H. Tsai, H. J. Wang, Y. C. Kuo, T. K. Yeh, C. S. Yang and P. Lin, *Environ. Health Perspect.*, 2007, **115**, 1339–1343.
25 Z. Chen, H. Chen, H. Meng, G. Xing, X. Gao, B. Sun, X. Shi, H. Yuan, C. Zhang, R. Liu, F. Zhao, Y. Zhao and X. Fang, *Toxicol. Appl. Pharmacol.*, 2008, **230**, 364–371.
26 Y. Su, F. Peng, Z. Jiang, Y. Zhong, Y. Lu, X. Jiang, Q. Huang, C. Fan, S. T. Lee and Y. He, *Biomaterials*, 2011, **32**, 5855–5862.